The 2010 IEEE/RSJ International Conference on
Intelligent Robots and Systems
October 18-22, 2010, Taipei, Taiwan

RobOtol : From Design to Evaluation of a Robot for Middle Ear Surgery

Mathieu Miroir[1], Yann Nguyen[1] M.D., Jérôme Szewczyk[2], Stéphane Mazalaigue[3], Evelyne Ferrary[1,4] M.D., Olivier Sterkers[1,4,5] M.D. and Alexis Bozorg Grayeli[1,4,5] M.D.

Abstract— **Middle ear surgery requires micro-surgical techniques and may benefit from robotic assistance. A prototype of tele-operated system is presented. Methods to determine design specifications, kinematic structure and optimization of the micro-manipulator are described. First evaluation of the robot by a stapedial removal through the external auditory meatus in human temporal bone specimens, simulating the surgery of otosclerosis, is presented. In this procedure, the robot yielded accessibility to the target area with a reduced visual impairment and, an enhanced tool stability compared to the surgeon's hand.**

I. INTRODUCTION

Surgical techniques are expected to be significantly improved with the development of high-tech surgical tools [1]. The experience in robotic or tele-operated systems is now growing in laparoscopic surgery and endoscopic pharyngolaryngeal surgery [2], [3]. However, there is no robotic device commercially available for microsurgery. This technique refers to procedures under operating microscope such as those carried out in otology, neurosurgery, ophthalmology, plastic surgery or orthopedic surgery. Accurate positioning, sub-millimetric displacements, tremor filtration, and preservation of the visual field are the principal objectives for robotic assistance in microsurgery. While the da Vinci system (Intuitive Surgical Inc., Sunnyvale, CA) can enhance the surgeon's motor capabilities in laparoscopic surgery, this robot is poorly adapted to microsurgery due to its dimensions, kinematics and tools. Few prototypes have been designed for ophthalmologic or middle ear surgery [4]. Their specifications correspond to a rather limited field of surgical functions [4]. These protoypes have in common an high resolution in displacement necessary to microsurgery [5], [6], and [7]. However, the preservation of visual field, a critical specification in ear surgery, is seldom taken into account. During eye or platic surgery, the visual field is ussually wider than in middle ear surgery.

The auditory organ is a functional chain that can be decomposed into several zones : in external ear (pinna, external ear canal), middle ear (tympanic membrane, middle ear cleft containing 3 ossicles: malleus, incus, and stapes), inner ear (cochlea), auditory nerve, brainstem, and auditory cortex. Middle and inner ear are located in the temporal bone. Causes of hearing loss can be divided into conductive concerning mainly the external and middle ears, and sensorineural originating from cochlea or the central nervous system. Middle ear surgery has been developed for a century and is now routinely practiced for conductive hearing loss. Most of the procedures consist of tympanic membrane grafts or ossicular chain replacement with a prosthesis. Among these procedures, otosclerosis surgery, which is the most delicate [8], was chosen as a procedure objective for the development of our robotic system. This procedure is highly reproducible in different patients and by different surgeons. Otosclerosis is a bone dystrophy leading to a stapes fixation, impairing its vibration and the sound transmission to the inner ear (Fig. 1 and Fig. 2(a)).

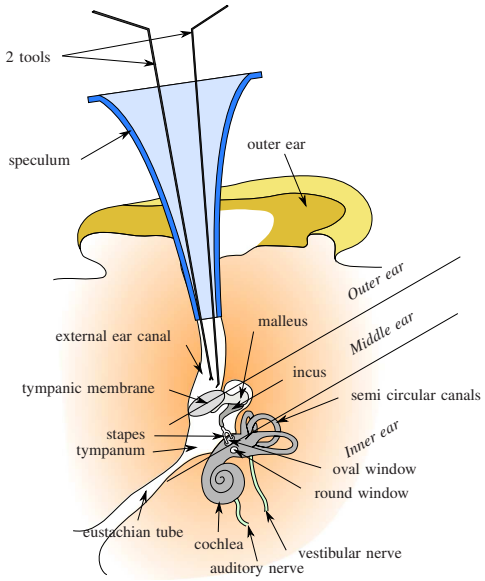

Fig. 1. Human ear

The treatment consists of the stapedial superstructure resection, the fenestration or the removal of the stapes footplate, and the placement of an ossicular prosthesis between the incus and the fenestrated stapes to restore the conductive properties of the middle ear [9] (Fig. 2(b)). The procedure is performed through a speculum in the external auditory canal which represents a narrow operation field. The exposure is also reduced because the middle ear approach through the external auditory canal has a tunnel shape, and the surgeon has to handle the tools parallel to the vision axis. To expose the stapes, it is usually necessary to drill the posterior-

[1] UMR-S 867 Inserm / Université Paris 7 Denis Diderot, Paris, France
[2] ISIR, CNRS UMR 7222, Université Paris 6 P. et M. Curie, Paris, France
[3] Collin Inc, Bagneux, France
[4] AP-HP, Hôpital Beaujon, service ORL, Clichy, France
[5] Université Paris 7 Denis Diderot, Paris, France
Corresponding address : mathieu.miroir@inserm.fr

superior rim of the external ear canal in its medial part. Low interaction forces (<1 N) occur between the tool and the ossicular chain and their light variation cannot be easily perceived by the surgeon [10]. Thus, functional success and hearing loss improvement is related to the surgeon's dexterity and experience [11]. Partial or complete hearing gain can be observed in 90% of cases [8]. However, surgery can be complicated by a complete and irreversible hearing loss in 0.2 to 3% of the cases [12]. Therefore a robotic assistance could improve precision and safety of the procedure.

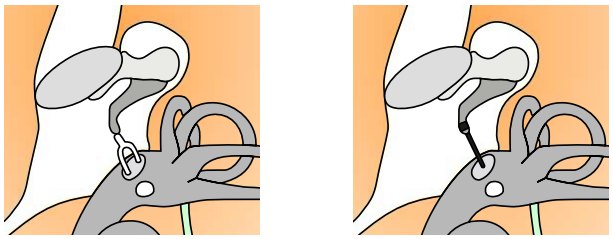

(a) (b)

Fig. 2. Human middle ear with preoperative view (a) and postoperative otosclerosis surgery (b)

Other reported works in the field of otosclerosis surgery focused on the stapedial fenestration and prosthesis crimping around the incus. Baker reported the requirements for a robotized drilling tool to fenestrate the stapedial footplate [13]. They monitored force, torque, and displacement in order to detect the breakthrough of the stapes and to stop the drill. A similar robot was designed and assessed for an atraumatic cochleostomy (opening of the cochlea) [14]. A co-manipulated robot designated "the steady hand" was used to perform a micro-pick fenestration. Authors observed a reduction of the cumulative force by 31 Ns [10] (-58%) and of the maximum force by 1.08 N (-17%) applied to the stapes footplate in comparison to the standard technique. They also noted a decrease of the maximum force applied for crimping the prosthesis [15]. The aim of this study was to design an optimal system dedicated to the middle ear surgery. A prototype of an assistance robot for the microsurgery of the middle ear designated as "RobOtol" is presented. Determination of design specifications, optimization, prototyping, and evaluation of this prototype in human temporal bone specimens will be described.

II. DESIGN SPECIFICATIONS

The initial step of the project was to define the design specifications. For the stapes surgery, we decided that the surgeon will be positioned at the head of the patient and will control the procedure under the operating microscope similarly to an unassisted procedure. Consequently, the extra-corporeal environment composed of the microscope, the patient's head and upper thorax and the operating table was defined and measured. The first objective was to prevent collision between the robot and the extra-corporeal environment, and preserve the visibility of the surgical field. We chose to enable the robot's base and the microscope to move freely around the patient's head in order to allow multiple position configurations and to increase the possibility of the robot's use in different procedures. Consequently, we defined a planar model (Fig. 3(a)) with a revolution around the view axis (Fig. 3).

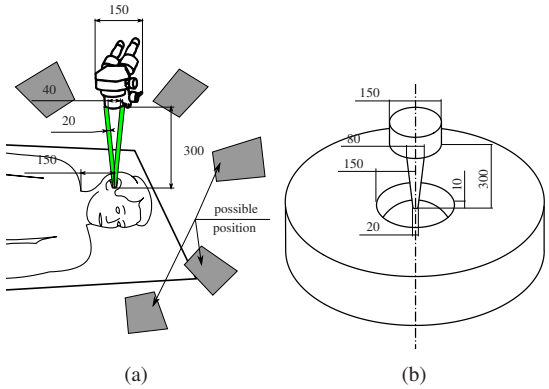

(a) (b)

Fig. 3. Extra-corporeal space assessment (dimensions in mm)

Another requirement concerned the internal workspace (Fig. 4) : The tool's tip should access all the space within the speculum, the external auditory canal and the visible part of the middle ear cleft. A geometrical approximation (Fig. 4(a)) with a simple shape allowed us to maximize this workspace. The cylinder A included the auditory canal and the visible part of middle ear cleft and the cone B, the speculum. We measured on 12 consecutive patients the maximum diameter and the height of the volume A by using 3-dimensional multi-planar reconstructions on computed tomography [16] and considered the highest values for defining the workspace dimensions.

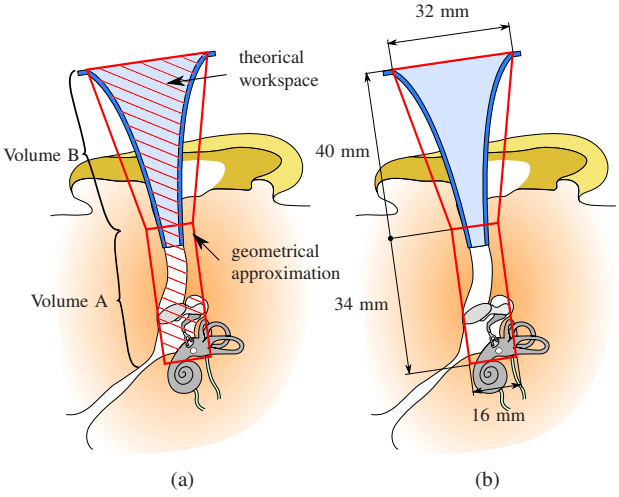

(a) (b)

Fig. 4. Modelized workspace

Forces necessary to perform various steps of middle ear surgery had also to be specified . Few data were available in the literature ([10], [15] and [17]). For this purpose, a specific test bench was designed (Fig. 5) allowing the surgeon to simulate surgical gestures with real tools in a realistic environment. Otologic surgeons performed surgery on 8 human

temporal bone specimens. Applied forces on temporal bone during mastoidectomy, external auditory canal bone drilling and stapedial footplate fenestration were measured by a 6-axis force sensor mounted under the specimen (ATI nano 43, ATI Industrial Automation, Apex, NC). The highest value required to achieve these tasks (5 N) was considered a robot specification [16].

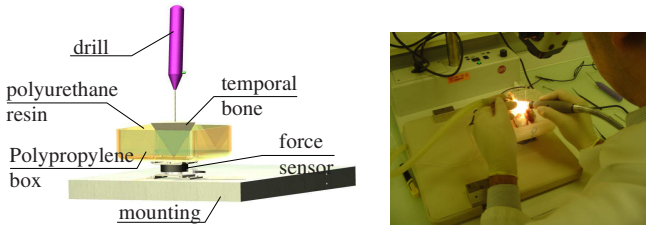

Fig. 5. Force measurement

Finally, the precision of robot displacements was set at 1% of the position or the shape of stapedial fenestration. The size of this fenestration was considered to be 0.5 mm, and a geometrical computation (Fig. 6) led to a linear resolution of 5 μm and an angular resolution of 8°.

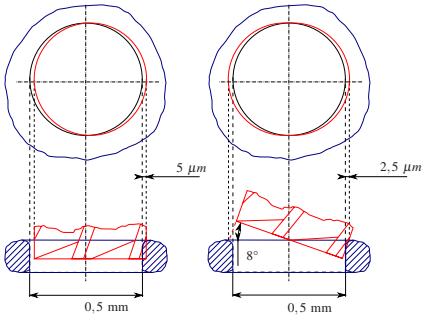

Fig. 6. Resolution required

III. DESIGN OPTIMISATIONS

Considering the shape of the workspace, a kinematic chain with 6 degrees of freedom, composed of 3 perpendicular linear links at its base and 3 rotary links at the distal part was selected. In order to obtain a tool rotation around its distal extremity, the axes of the 3 last links were designed to obtain a Remote Center of Motion at that point [18], [19]. The kinematic diagram and its parameters are presented in Fig. 7. In this particular kinematic, translational and rotational motion were uncoupled.

The next step was to optimize the parameters as a function of design specifications. Each candidate was defined by a set of parameters. Then each candidate was evaluated for multiple criteria and compared with all others [20].

First, tool positions with maximum angles, representing the most complex trajectory of the tool, were assessed. These positions represented the sweeping of the tip of the tool on the upper surface of the volume A in 30 configurations (Fig. 8(a)). For each configuration, the lateral part of the tool had to follow the upper surface of the volume B in 9 steps (Fig. 8(b)). Then, for each of these configurations, the tool had to be able to turn around its axis in 9 steps (Fig. 8(c)). This 6D trajectory represented in Fig. 8 had 2433 configurations with 3 approach configurations of the tool.

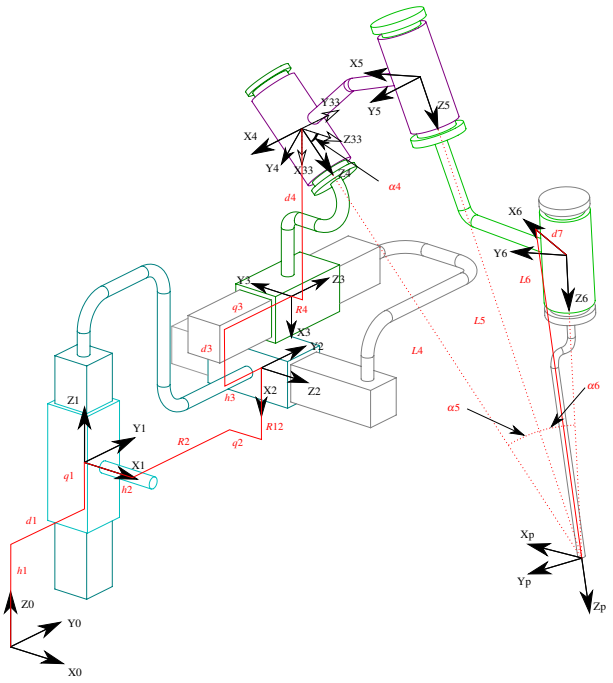

Fig. 7. Kinematic diagram and parameters

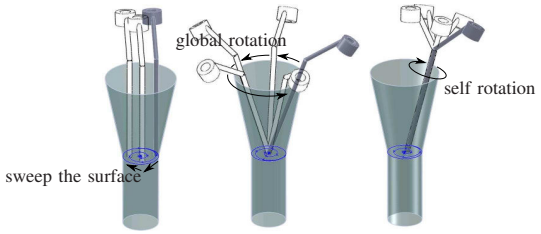

Fig. 8. Tool trajectory in optimization process. (a): sweeping surface, (b): rotation with a fixed tip of tool, (c): Rotation around tool axis

Then, each candidate was tested with equation (1) to determine the joint coordinates enabling the robot arm to reach every point of the previously described trajectory [21], [22].

$$d_x = \begin{bmatrix} \overrightarrow{d_p} \\ \overrightarrow{d_\theta} \end{bmatrix} = \begin{bmatrix} \overrightarrow{p} - \overrightarrow{p} \\ \frac{1}{2}(\overrightarrow{n} \wedge \overrightarrow{n} + \overrightarrow{o} \wedge \overrightarrow{o} + \overrightarrow{a} \wedge \overrightarrow{a}) \end{bmatrix} \quad (1)$$

Where d_x is the space displacement from the current configuration (represented by the homogeneous transformation matrix T_0^p) to the required configuration (represented by the homogeneous transformation matrix $\tilde{T}_0^p$).

$$\tilde{T}_0^p = \begin{bmatrix} \tilde{n}_x & \tilde{o}_x & \tilde{a}_x & \tilde{p}_x \\ \tilde{n}_y & \tilde{o}_y & \tilde{a}_y & \tilde{p}_y \\ \tilde{n}_z & \tilde{o}_z & \tilde{a}_z & \tilde{p}_z \\ 0 & 0 & 0 & 1 \end{bmatrix} \quad , \quad T_0^p = \begin{bmatrix} n_x & o_x & a_x & p_x \\ n_y & o_y & a_y & p_y \\ n_z & o_z & a_z & p_z \\ 0 & 0 & 0 & 1 \end{bmatrix}$$

For each configuration, the distance to the environment and the percentage of free vision were computed as shown in Fig. 9. The smallest distance (Fig. 9(a)) and the average percentage of free vision (Fig. 9(b)) graded the candidate.

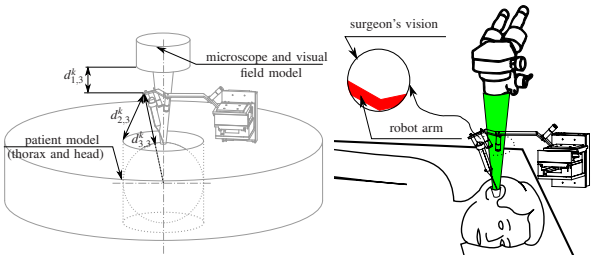

(a) (b)

Fig. 9. Modelization of distance to environment (a) and free vision under surgical microscope (b)

In order to comply with the pre-established specification for actuator ability to produce 5 N at the extremity of the tool in all directions, the required force of each actuator was evaluated with static equations in each configuration. The highest value was considered to choose the actuators. Optimization resulted in a Pareto's front of solutions (Fig. 10). Among these solutions, the candidate (n°110) with the highest distance to the external environment was selected to maximize security.

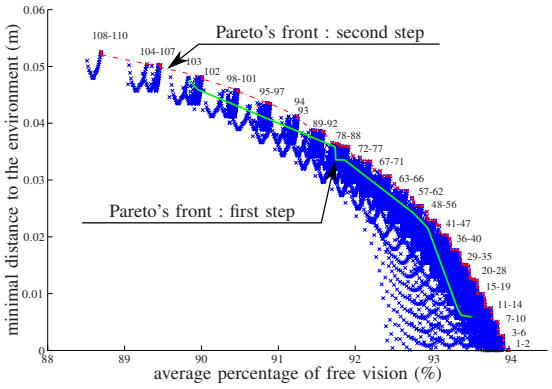

Fig. 10. Optimization results and candidate selection

IV. SYSTEM IMPLEMENTATION

A. Components

Linear actuators were selected considering the necessary stroke, resolution and force. A XYZ cross table was built with two orthogonal (X-Y) precision linear stages with a 70 mm travel, orthogonal to a precision linear Z-stage with a 95 mm travel (OWIS: LTM 80P-75-HSM and OWIS: LTM 80P-100-HSM, OWIS GmbH, Staufen, Germany). These linear stages were parallel mounted, 2 phase step motors, had a hall-effect limit switches and were economically priced. The resolution of these stages is 0.5 μm and the actuating force is 50 N.

Rotary actuators were selected depending on torque, weight, and cost. We chose the same DC micromotor (Faulhaber: 2342S024CR, Faulhaber GmbH, Germany) with magnetic incremental encoder IE2-512 (512 lines per revolution) for all rotary actuators. These were connected to a Harmonic Drive gearhead (Harmonic Drive: HFUC-8-50-2A-R, Harmonic Drive LLC, Peabody, MA) with a 50:1 reduction ratio.

The two last actuators were placed remotely in order to keep the arm of the manipulator as slim as possible. The movements from the actuators to the axis were transmitted by Bowden cables [23]. This transmission had the advantage of being light and simple to integrate in the robotic arm.

B. Command

We chose a tele-operated method to command this robot. The main reason was to keep the operating space around the patient's ear free. The Phantom Omni (SensAble Technologies, Inc., Woburn, MA) interface was used as a master arm. In order to have a simple and intuitive master arm, the command was based on a registration between the local frame of the stylus and the robotic arm frame (Fig. 11(a)). This coupling mode allowed the operator to overcome the permanent correspondence between the relative positions of the master and the robotic arm. It could also resolve a potential eye-hand incoordination if an indirect vision feedback was provided (i.e., angled endoscope). A velocity command was implemented. To move the tool, the surgeon defined an origin position and orientation by pushing the interface button before displacing the stylus. A differential computation was performed between the new current stylus position and the original configuration (using equation (1)). The result was projected and sent to the robotic arm to perform the displacement (Fig. 11(b)). A higher amplitude of stylus movement led to a higher speed of the robotic arm. To stop the displacement the surgeon had to release the interface button.

V. EVALUATION

The primary objective was to assess the ability of the tool to reach the whole workspace with a preserved visual field, and hence validate the design specifications, the choice of the kinematic structures, components, and the optimization. The secondary objective was to realize a simple task such as stapes removal. During the last part of the study we tested the possibility of adding an 30° endoscope in the visual field in order to modify the surgical approach to the middle ear. The robotic arm was evaluated by a senior ENT surgeon in 3 fresh temporal bones. The robotic device was placed in front of the surgeon. The surgery was performed by a transcanal approach similar to clinical practice. To perform the tasks,

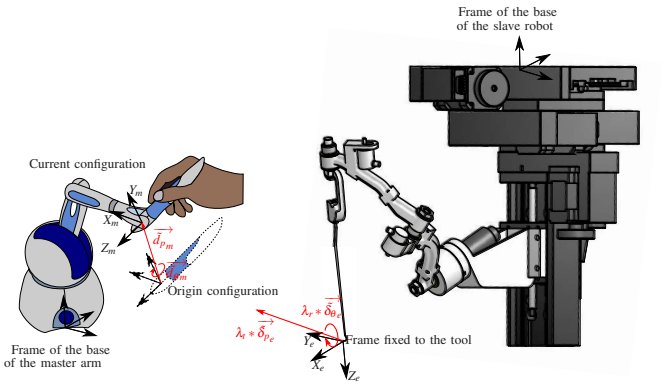

(a)

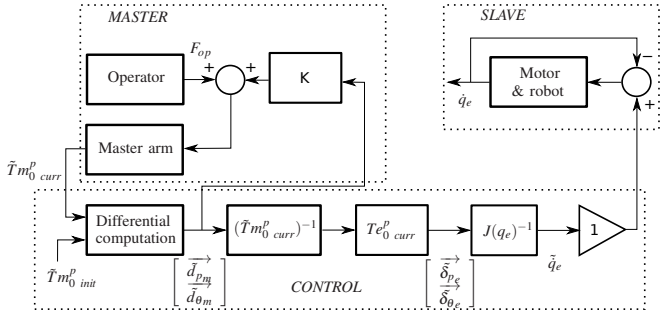

(b)

Fig. 11. Controller process and structure

a 90° angled micro-hook was mounted on the robotic arm. Direct vision was provided by a microscope with a 400 mm focal lens (Carl Zeiss, Jena, Germany). The master arm was placed under the surgeon's right hand (Fig. 12).

Fig. 12. Evaluation of RobOtol in a temporal bone

A. Entire workspace accessibility and visual field integrity

1) Material and methods: The objective of this step was to reach each of the four quadrants of the tympanic membrane, and after the tympanic membrane displacement, the stapes footplate, and the round window in the middle ear cleft under permanent visual control. Visual field integrity was assessed by per-operative microscope images analysis with ImageJ (http://rsbweb.nih.gov/ij/). Photos of the surgery with the robotic arm were compared with photos extracted from real surgery movies for percentage of free visual field.

2) Results: The surgeon was able to tele-operate the tool to reach all the targets with an appropriate accuracy corresponding to the accuracy expected and required during real surgery (Fig. 13). In addition, anatomical regions (posterior part of the tympanic cavity: sinus tympani) impossible to reach during real surgery due to the human wrist limitation were accessed with the robotic tool since RobOtol allowed an anterior-posterior direction of the micro-hook. During the tool displacement no singularity configurations were reached.

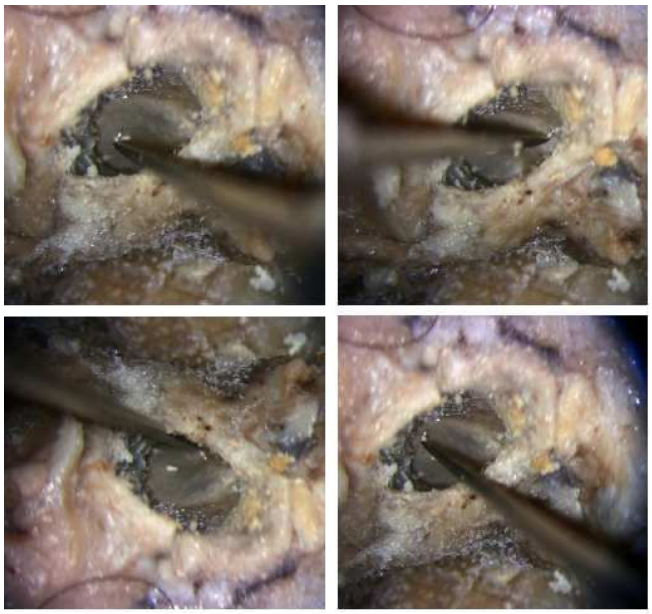

Fig. 13. Workspace access. All four quadrants of the tympanic membrane were accessed with a preserved visual field

In unassisted surgical conditions (extracted from real surgery movies), visual field was significantly impaired by the tool and the surgeon's hand holding the tool in the axis of the microscope aligned with the speculum. The measured free visual field represented 63.5 % of the speculum diameter. Using the robotic arm, only the tool impaired the visual field. Therefore the measured free visual field was greatly enhanced and represented 91.8 % of the speculum diameter (Fig. 14).

B. Stapes removal and robot - endoscopic assisted surgery evaluation

1) Material and methods: Stapes removal was conducted through a transcanal approach with two types surgical field visualization. In the first setting, exposure was obtained with the microscope after scutum lowering. In the second setting, it was obtained with a 30° angled, 4 mm diameter endoscope (KARL STORZ GmbH, Tuttlingen, Germany) maintained by a fixed articulated arm (Fig. 15). During the endoscopic procedure, no scutum lowering was necessary. Procedure was

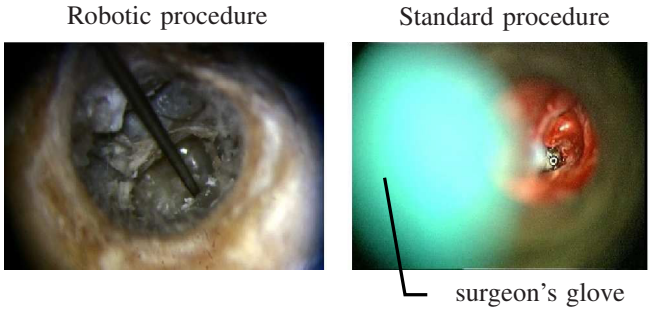

Fig. 14. Intra-operative visual field in a robot assisted technique (left) and in a standard technique (right). Free visual field is enhanced in the robotic procedure

considered achieved if the stapes could be extracted without any damages to surrounding anatomical structures (incus, facial nerve, and cochlea).

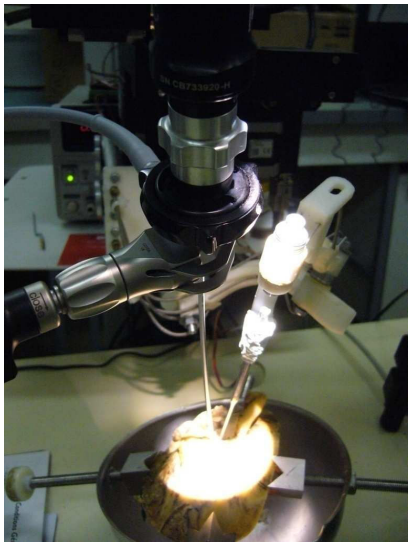

Fig. 15. Simultaneous use of the robotic arm and a 4 mm endoscope in the external auditory canal

2) Results: Stapes removal was performed successfully with the microscope and with the endoscope (Fig. 16). No lesion to the other anatomical structures was observed. The low overall dimensions of the robotic arm allowed an easy access and surgical gesture in the middle ear cleft.

C. Discussion

During evaluation, all objectives were reached since the surgeon was able to command the robotic arm and reach the entire workspace. The visual field was enhanced in the robot-assisted procedure. A simple task such as stapes removal could be performed safely. Simultaneous use of the endoscope and the robotic arm was possible. These observations validated the technological design of our prototype.

Middle ear surgery requires microsurgery skills as anatomical structures have millimetric dimensions. Robotic assistance can enhance surgeon's dexterity to reduce tremor, jerk, drift and overshoot [24].

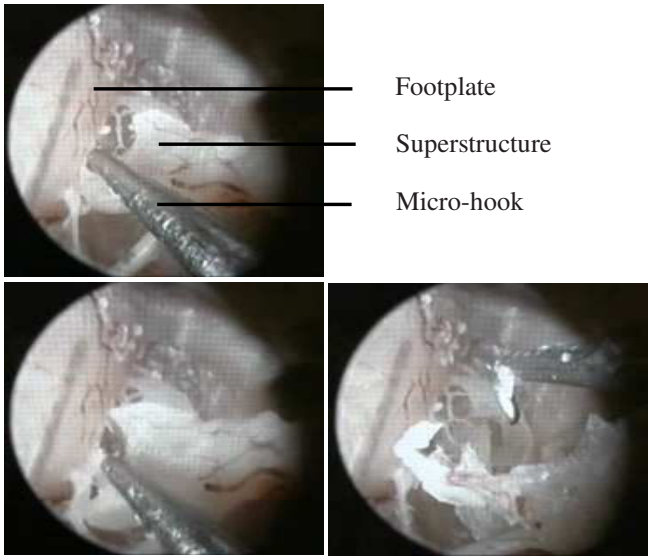

Fig. 16. Stapes removal under endoscopic procedure

Benefits for the patients are multiple. First, it can provide more security to the procedure with a lower risk of lesion to the surroundings anatomical structures. Moreover, surgical functional results could be enhanced by a smoother, a more accurate, and a more reproducible fenestration, prosthesis positioning and crimping. Finally, the robotic assisted procedure is potentially faster and less invasive since it will lead to a simplified surgical gesture and procedure.

The other issue in middle ear surgery is the operating field exposure. Vision provided by the microscope is aligned with the external ear canal which has a small diameter (less than 6 mm diameter). Wider exposure is possible but requires ear canal bone drilling and could hamper tympanic membrane closing. To enhance dexterity and reduce tremor, surgeons have to hold the instruments closer to the tip, and to stabilize their hands on patient's head around the speculum. Thus, up to one third of this small visual field can be hidden by the surgeon's hand and tools. In contrast, the robotic arm holds the tool far from the tip and interferes much less with the vision. Another possibility tested was the use of an endoscope with the robotic arm. Endoscopes are used in middle ear surgery to explore the middle ear cleft and can expose all the recesses thanks to the angled optical lens. They are usually used for diagnostic or control during the procedure rather than for surgical treatment because the angled vision hampers the eye-hand coordination. Our prototype and command settings offer the possibility of a referential readjustment and overcome the eye-hand shift issue. With our command settings , it makes no difference for the surgeon if he is working with a straight, 30° or 70° angled endoscope.

Moreover, the arm dimensions are small enough to travel all around the endoscope to perform the task. Thus the standard otosclerosis procedure requiring a scutum lowering can be refined to a less invasive technique by keeping the complete bone frame around the tympanic membrane.

VI. CONCLUSION AND FUTURE WORKS

Middle ear surgery has specific micro-surgical requirements and only few works have been conducted in this field. For our robot design, we chose the otosclerosis procedure as it is a reproducible surgery needing high accuracy. Our design was based on objective specifications related to tool-organ interactions in human temporal bone measurements, and extra- and intra-corporeal workspaces. Subsequently, we chose and optimized the kinematic structure and actuators. Finally, we evaluated the first prototype in human temporal bone showing the validity of our calculations and choices. Stapes removal was performed and surgical procedure was improved with the use of an endoscope. The next step is to design a full set of tools for the robotic arm in order to perform the full procedure. Duration and tool-organ interaction force will then be compared between manual and robotic-assisted technique per surgeons with different levels of experience.

REFERENCES

[1] I. Emeagwali, P. Marayong, J. J. Abbott, and A. M. Okamura, "Performance analysis of steady-hand teleoperation versus cooperative manipulation," in *Proceedings of the 12th International Symposium on Haptic Interfaces for Virtual Environment and Teleoperator Systems, IEEE Virtual Reality*, Chicago, IL, USA, 27-28 March 2004, pp. 316–322.

[2] J. Marescaux, J. Leroy, M. Gagner, F. Rubino, D. Mutter, M. Vix, S. E. Butner, and M. K. Smith, "Transatlantic robot-assisted telesurgery," *Nature*, vol. 413, no. 6854, pp. 379–380, 27 September 2001.

[3] B. W. O'Malley, Jr, G. S. Weinstein, W. Snyder, and N. G. Hockstein, "Transoral robotic surgery (tors) for base of tongue neoplasms," *The Laryngoscope*, vol. 116, no. 8, pp. 1465–1472, 2006.

[4] B. Mitchell, J. Koo, I. Iordachita, P. Kazanzides, A. Kapoor, J. Handa, G. D. Hager, and R. H. Taylor, "Development and application of a new steady-hand manipulator for retinal surgery," in *ICRA 07 : International Conference on Robotics and Automation*. Roma, Italy: IEEE, 10-14 April 2007, pp. 623–629.

[5] W. Wei, R. Goldman, N. Simaan, H. Fine, and S. Chang, "Design and Theoretical Evaluation of Micro-Surgical Manipulators for Orbital Manipulation and Intraocular Dexterity," in *2007 IEEE International Conference on Robotics and Automation*, Roma, Italy, 2007, pp. 3389–3395.

[6] K. W. Grace, "Kinematic design of an ophthalmic surgery robot and feature extracting bilateral manipulation," Ph.D. dissertation, Northwestern University, Evanston, Illinois, 1995.

[7] P. S. Jensen, K. W. Grace, R. Attariwala, J. E. Colgate, and M. R. Glucksberg, "Toward robot-assisted vascular microsurgery in the retina," in *Graefe's Archives for Clinical and Experimental Ophthalmology*, vol. 235. Springer-Verlag, 1997, pp. 696–701.

[8] J. J. Shea, Jr., "Forty years of stapes surgery," *Otology & Neurotology*, vol. 19, no. 1, pp. 52–55, January 1998.

[9] Y. Nguyen, A. Bozorg Grayeli, R. Belazzougui, M. Rodriguez, D. Bouccara, M. Smail, and O. Sterkers, "Diode laser in otosclerosis surgery : First clinical results," *Otology & Neurotology*, vol. 29, no. 4, pp. 441–446, June 2008.

[10] D. L. Rothbaum, J. Roy, D. Stoianovici, P. J. Berkelman, G. D. Hager, R. H. Taylor, L. L. Whitcomb, H. W. Francis, and J. K. Niparko, "Robot-assisted stapedotomy : Micropick fenestration of the stapes footplate," *Otolaryngology – head and neck surgery*, vol. 127, no. 5, pp. 417–426, November 2002.

[11] D. L. Rothbaum, J. Roy, G. D. Hager, R. H. Taylor, L. L. Whitcomb, H. W. Francis, and J. K. Niparko, "Task performance in stapedotomy : Comparison between surgeons of different experience levels," *Otolaryngology – head and neck surgery*, vol. 128, no. 1, pp. 71–77, 2003.

[12] H. P. House, M. R. Hansen, A. A. Al Dakhail, and J. W. House, "Stapedectomy versus stapedotomy: comparison of results with long-term follow-up," *The Laryngoscope*, vol. 112, no. 11, pp. 2046–2050, 2002.

[13] D. A. Baker, P. N. Brett, M. V. Griffiths, and L. Reyes, "Surgical requirements for the stapedotomy tool : data and safety considerations," in *Proceedings of the 18th Annual International Conference of the IEEE Engineering in Medicine and Biology Society*, vol. 1. Amsterdam, Netherlands: Elsevier, 31 Oct-3 Nov 1996, pp. 214–215.

[14] C. J. Coulson, R. P. Taylor, A. P. Reid, M. V. Griffiths, D. W. Proops, and P. N. Brett, "An autonomous surgical robot for drilling a cochleostomy: preliminary porcine trial," vol. 33, pp. 343–347, 18 august 2008.

[15] P. J. Berkelman, D. L. Rothbaum, J. Roy, S. Lang, L. L. Whitcomb, G. D. Hager, P. S. Jensen, , R. H. Taylor, and J. K. Niparko, "Performance evaluation of a cooperative manipulation microsurgical assistant robot applied to stapedotomy," in *MICCAI 01 : Proceedings of the 4th International Conference on Medical Image Computing and Computer-Assisted Intervention*. London, UK: Springer-Verlag, 2001, pp. 1426–1429.

[16] M. Miroir, J. Szewczyk, Y. Nguyen, S. Mazalaigue, and O. Sterkers, "Design of a robotic system for minimally invasive surgery of the middle ear," in *Biorob 08 : Proceedings of the 2nd Biennial IEEE/RAS-EMBS International Conference on Biomedical Robotics and Biomechatronics*, Scottdale, AZ, USA, 19-22 october 2008, pp. 747–752.

[17] B. Plinkert and P. K. Plinkert, "Robotics in skull base surgery," *International Congress Series Computer Assisted Radiology and Surgery*, vol. 1230, pp. 138–142, June 2001.

[18] R. H. Taylor, J. Funda, B. Eldridge, S. Gomory, K. Gruben, D. LaRose, M. Talamini, L. Kavoussi, and J. Anderson, "A telerobotic assistant for laparoscopic surgery," *Engineering in Medicine and Biology Magazine*, vol. 14, no. 3, pp. 279–288, May/June 1995.

[19] G. Zong, X. Pei, J. Yu, and S. Bi, "Classification and type synthesis of 1-dof remote center of motion mechanisms," *Mechanism and Machine Theory*, vol. 43, no. 12, pp. 1585–1595, 2008.

[20] M. J. Lum, J. Rosen, M. N. Sinanan, and B. Hannaford, "Kinematic optimization of a spherical mechanism for a minimally invasive surgical robot," in *ICRA 04 : International Conference on Robotics and Automation*, 2004.

[21] R. P. Paul, *Robot Manipulators : Mathematics, Programming, and Control*. Cambridge, MA, USA: MIT Press, 1982.

[22] L. Sciavicco and B. Siciliano, *Modelling and Control of Robot Manipulators*. McGraw Hill, 1996.

[23] A. Schiele, P. Letier, R. Van Der Linde, and F. C. T. Van Der Helm, "Bowden cable actuator for force-feedback exoskeletons," in *IROS 06 : International Conference on Intelligent Robots and Systems*. Beijing, China: IEEE, 9-15 October 2006, pp. 3599–3604.

[24] S. Charles, "Dexterity enhancement for surgery," *Computer Integrated Surgery: Technology and Clinical Applications, ed. Taylor RH, Lavallee S, Burdea GC, et Mosges R*, pp. 467–471, 1996.